RI 9071

Bureau of Mines Report of Investigations/1987

Capability Evaluation of the Radial-Axial Splitter

By S. J. Anderson and D. E. Swanson

UNITED STATES DEPARTMENT OF THE INTERIOR

Report of Investigations 9071

Capability Evaluation of the Radial-Axial Splitter

By S. J. Anderson and D. E. Swanson

UNITED STATES DEPARTMENT OF THE INTERIOR
Donald Paul Hodel, Secretary

BUREAU OF MINES
Robert C. Horton, Director

Library of Congress Cataloging in Publication Data:

Anderson, Sterling J.
Capability evaluation of the radial-axial splitter.

(Report of investigations ; 9071)

Bibliography: p. 18.

Supt. of Docs. no.: I 28.23:9071.

1. Rock splitters (Machines). 2. Mining machinery—Testing. I. Swanson, David E. II. Title. III. Series: Report of investigations (United States. Bureau of Mines) ; 9071.

TN23.U43 [TN345] 622 s [622'.3] 86-600353

CONTENTS

ILLUSTRATIONS

TABLES

UNIT OF MEASURE ABBREVIATIONS USED IN THIS REPORT

ft	foot	kg	kilogram
g	gram	lb	pound
g/cm^3	gram per cubic centimeter	pct	percent
gpm	gallon per minute	psi	pound per square inch
in	inch		

CAPABILITY EVALUATION OF THE RADIAL-AXIAL SPLITTER

By S. J. Anderson[1] and D. E. Swanson[1]

ABSTRACT

To define the capabilities of a nonexplosive excavation concept, the Bureau of Mines conducted reduced-scale laboratory tests of a mechanical excavation tool called a rock splitter. The splitter investigated was capable of applying combinations of radial and axial loads to rock when placed in a predrilled hole. Experiments conducted with the tool in concrete, limestone, and granite proved it capable of excavating all three materials. Break geometry in these three materials was the same, which encourages the prediction of performance in all rocks. The design of the radial-axial loading splitter's feather components significantly affected the tool's performance. It appears the design of this in-hole component should be tailored for the rock to be excavated.

[1]Mining engineer, Twin Cities Research Center, Bureau of Mines, Minneapolis, MN.

INTRODUCTION

Investigations were conducted by the Bureau of Mines to further determine and optimize the operational and design characteristics of radial-axial loading splitters. These splitters are the heart of a nonexplosive-excavation concept having wide potential for use in underground mining and, as such, are part of a larger Bureau effort to evaluate new mining techniques.

Cost-effective splitter mining technology would enhance the domestic underground mining industry by making available an excavation technique that is versatile and energy efficient, even in the hardest formations. As a replacement for blasting, this technology would eliminate blast shock and ground vibrations, dust and toxic fumes, flyrock, overbreak, and associated production delays.

The radial-axial loading splitters used in this investigation are improved versions of those used in previous Bureau studies (1).[2] Previous investigations determined that radial-axial loading splitters present a greater potential for use in underground mining than do other splitter types (2-4). Radial-axial loading splitters differ in that they generate fractures that propagate from an in-hole anchoring point back to the free surface of the working face. To accomplish this, the tool uses concentric in-hole components made up of a wedge, thrust rod, and feathers that are actuated by a special hydraulic cylinder (fig. 1). The improved splitter (fig. 2) has increased force output that enables operation at extended depths and in tougher materials. Experiments with this improved splitter were conducted in the laboratory at reduced scale and were expanded from operation in concrete (the only material fragmented in previous studies) to operations in limestone and granite.

EXPERIMENTAL PROGRAM

The experimental program was divided into three areas; the first optimized splitter design and focused on trials with an array of feathers that varied in geometry and metallurgy, the second analyzed splitter capabilities in limestone and granite, and the third investigated the splitter's operational characteristics.

Design optimization of the splitter concentrated on the feather portion of the tool's in-hole components. Because the feather interacts directly with the rock to be broken, it plays a key role in the fracturing process. As the experiments were conducted in the three materials, the effect that feather-design

[2]Underlined numbers in parentheses refer to items in the list of references preceding the appendix at the end of this report.

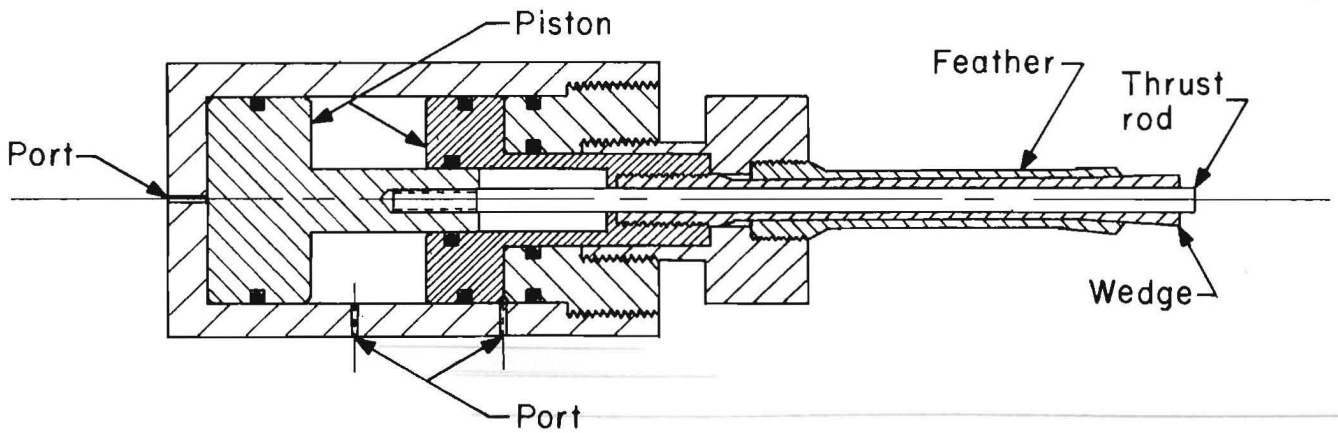

FIGURE 1.—Splitter cross section.

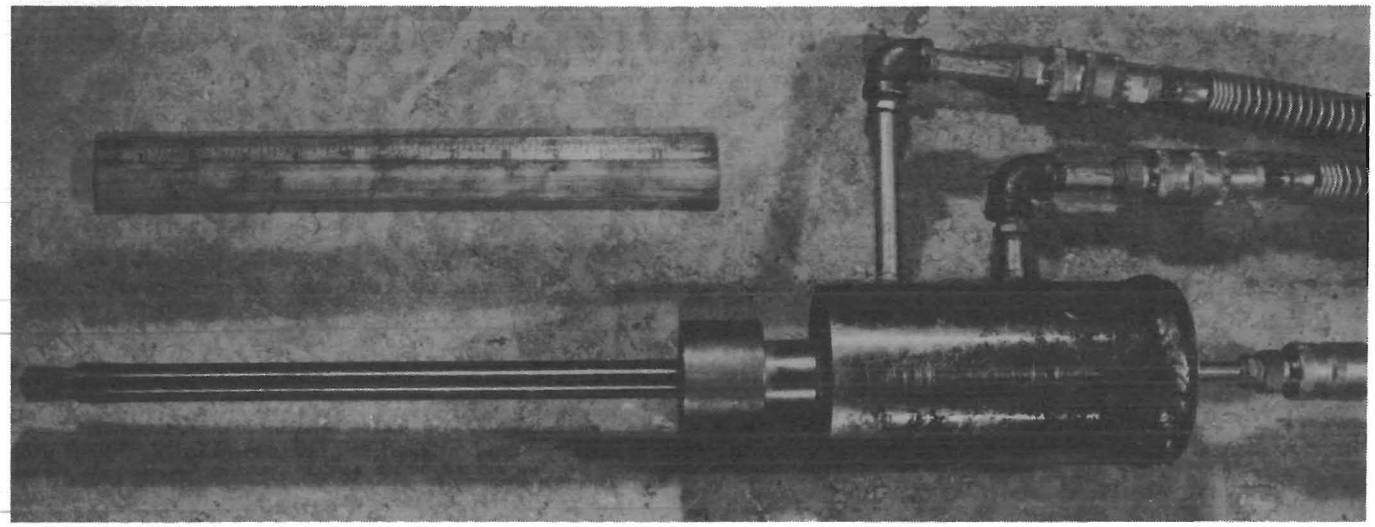

FIGURE 2.—Laboratory radial-axial loading splitter.

changes had on the forces required to produce breaks and on the quantity of material removed by the break, or the break effectiveness, was analyzed.

A predictive data base was produced by the second area of the experimental program. The variables investigated included depth of break, radial- and axial-force requirements, and break effectiveness. These experiments were run with respect to prepared planar surfaces of the two rock types. The resultant data were used for comparisons of performance.

The operational characteristics investigated included paired breaks, confinement, and tool orientation with the face and rock structure. With these experiments, tool-rock interaction was studied to determine the most efficient modes of breaking. Excavation of a simulated drift in limestone, and breaks made in the surfaces of the two rock types provided information in this area of investigation.

EQUIPMENT AND MATERIALS

The splitters used in this investigation had two major components: a hydrauliic-cylinder component containing two double-acting pistons capable of independent movement, and an assembly of in-hole components that connect with the pistons and the cylinder body itself.

The hydraulic cylinder individually actuates the wedge and thrust-rod portions of the in-hole components and thereby supplies the energy required to break rock. The in-hole components comprised of feathers, wedge, and thrust rod are the mechanical means by which the splitters generate breaks (fig. 3). Operating in a previously drilled hole, the wedge is drawn back into the feathers, forcing them outward aganist the hole wall, securely anchoring the splitter within the hole with a radial load. Once this is done, the thrust rod is extended. When contact is made with the hole bottom, an axial load is applied to the rock. The resulting strain imposed on the rock by the radial and axial loads causes the rock to fracture.

As a result of a designed increase in the size of the splitter cylinder, the force-generating capabilities of the splitters used in this investigation are greater than those previously used by the Bureau (1). The cylinder has a 2.50-in bore diameter, a maximum operating pressure of 2,400 psi, and can apply loads of up to 11,760 lb of force axially and up to 57,000 lb radially in conjunction with the feather and wedge portions of the in-hole components. Pressure transducers plumbed into the radial- and axial-pressure supply lines of the splitter

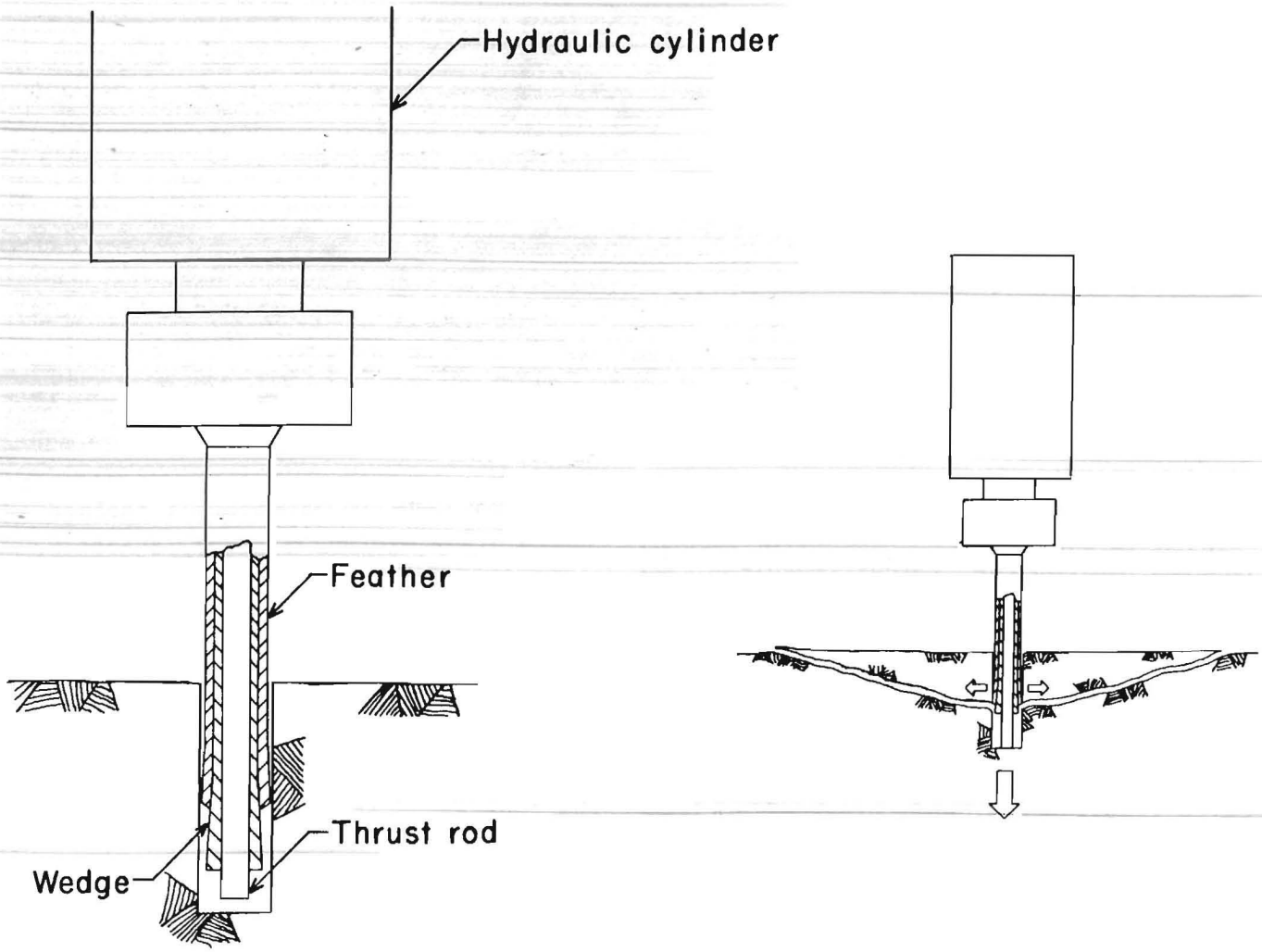

FIGURE 3.—In-hole components of the splitter (left) and break generation (right), indicated by arrows.

responded to the loads applied by the tool and sent their signals to strip-chart recorders for documentation. The radial and axial loads on the tools were calculated from these pressure readings.

In-hole component design is critical to the effective operation of the splitter. Because of the increased radial and axial force-generating capabilities, the in-hole components were enlarged and required a 0.875-in-diam hole within which to operate. Tool steels that were heat-treated for increased hardness and strength were used for these three concentric components.

The splitters were powered by an electrically driven hydraulic pump with output capabilities of .50 gpm and 3,000 psi. Control panels provided for the regulation of splitter-actuation speed, pressure, and direction of individual in-hole component movement. Sections of flexible 10-ft hydraulic hose connected the splitters to the control panels (fig. 4). Drilling required by the splitter was accomplished by an electrically powered, rotary-percussive, hand-held drill.

The materials fragmented in these experiments were concrete, limestone, and granite. The concrete was a sand, portland-cement mix, that was cast in cubic forms at the Twin Cities Research Center and given a minimum 90-day curing to ensure full strength prior to use. The limestone and granite were large blocks of dimension stone obtained from local quarries. The limestone was a banded yellow dolomitic quartz with thin white partings of dolomite. This sandy

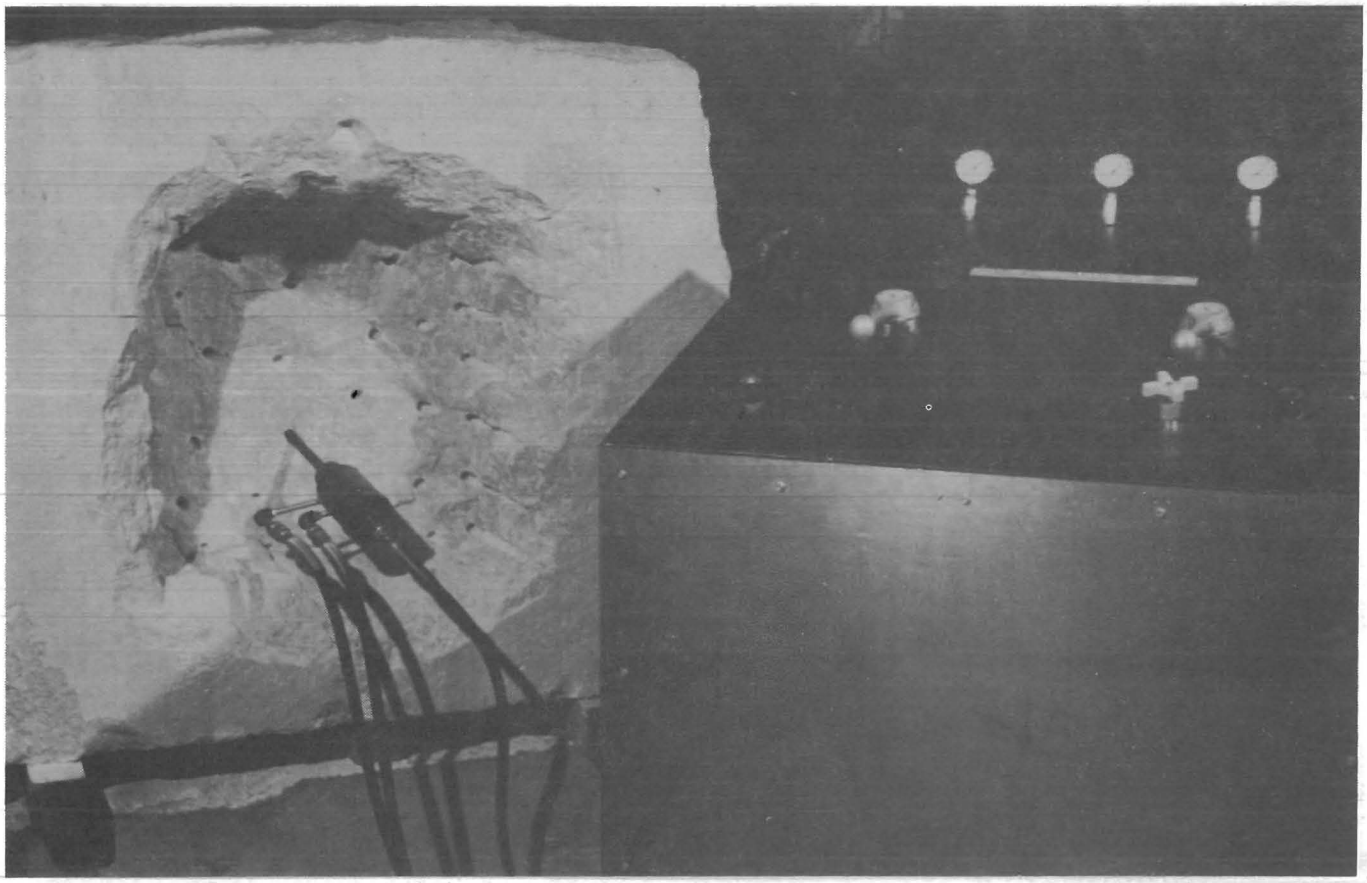

FIGURE 4.—Splitter connected to control panel.

dolestone was medium to fine grained with a silt-sized dolomitic matrix. Voids, pea-sized and smaller, were infrequently found in the stone. The granite was a dark-red, medium-grained, equigranular to porphyritic, gneissic quartz monzonite that contained approximately 5 pct biotite. Table 1 gives a more detailed description of the materials fragmented and some of their material properties.

TABLE 1. - Description and physical properties of material fragmented

Material	Description		Origin	Strength, psi		Apparent density, g/cm^3
	Geologic	Commercial		Compressive	Tensile	
Concrete[1]....	...NAp.....	Portland cement, 10-lb bag mortar mix; low water, fine sand; 3-in slump.	NAp.....	7,894	668	2.21
Limestone (5)	Oneonta Member, Prairie du Chien Formation.	Kasota stone.....	Kasota, MN.	13,000	580	2.48
Granite[1].....	Early Precambrian quartz monzonite.	Mahogany granite.	Ortonville, MN.	25,827	957	2.65

NAp Not applicable.
[1]Properties measured in the laboratory.

OPERATING PROCEDURES

The splitter's operating procedures were consistent from test to test throughout the experimental program. When operating on the face of the wire-sawed blocks, each break was spaced sufficiently to make it independent of previous breaks and the block's edges (fig. 5). In the simulated drift in limestone, breaks were not independent, but interacted with each other and were made successively over previous breaks as the drift advanced (fig. 6). Each hole required by the splitter was drilled to a predetermined surface alignment and depth. Drill-hole position was determined on the basis of break function, with respect to the experience gained by previous breaks, and on the characteristics of the rock being fractured.

After each break, cylinder pressures corresponding to the maximum radial- and axial-force loadings were recorded, as were the circumstances surrounding the break, the depth, the effectiveness, and any problems or peculiarities. Excavated break material was then gathered, weighed, and recorded.

RESULTS AND DISCUSSION

Both quantitative and qualitative analyses of the data generated from the experimental program are presented in the following subsections. Regression-analysis techniques were sometimes used to evaluate the data. As a check on the validity of these analyses, null-hypothesis testing was conducted according to Chatterjee (6). This test examines whether x explains a significant amount of variation in y. The confidence level in these evaluations was 95 pct. These data can be found in the appendix.

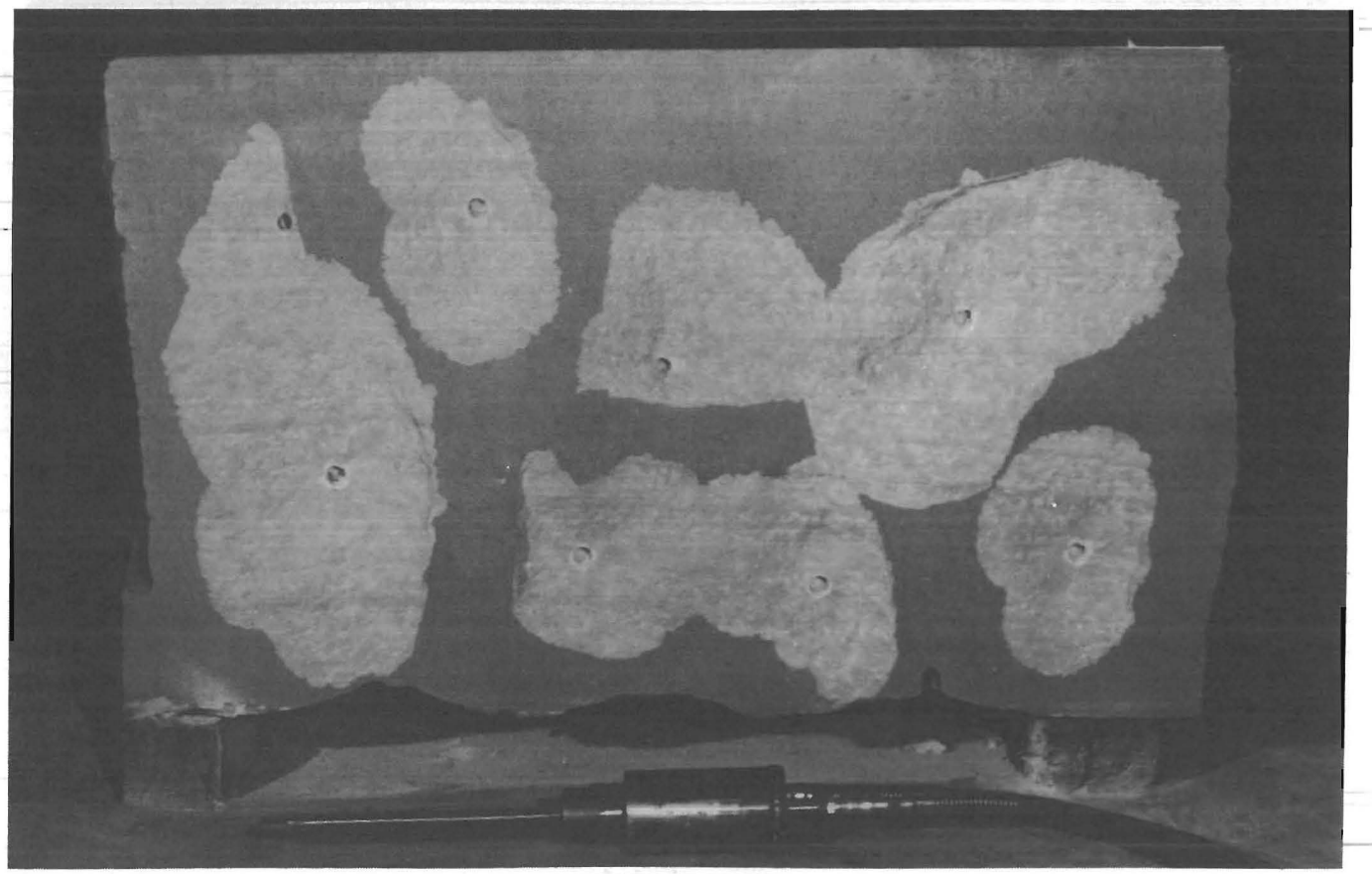

FIGURE 5.—Breaks spaced to insure independent tests.

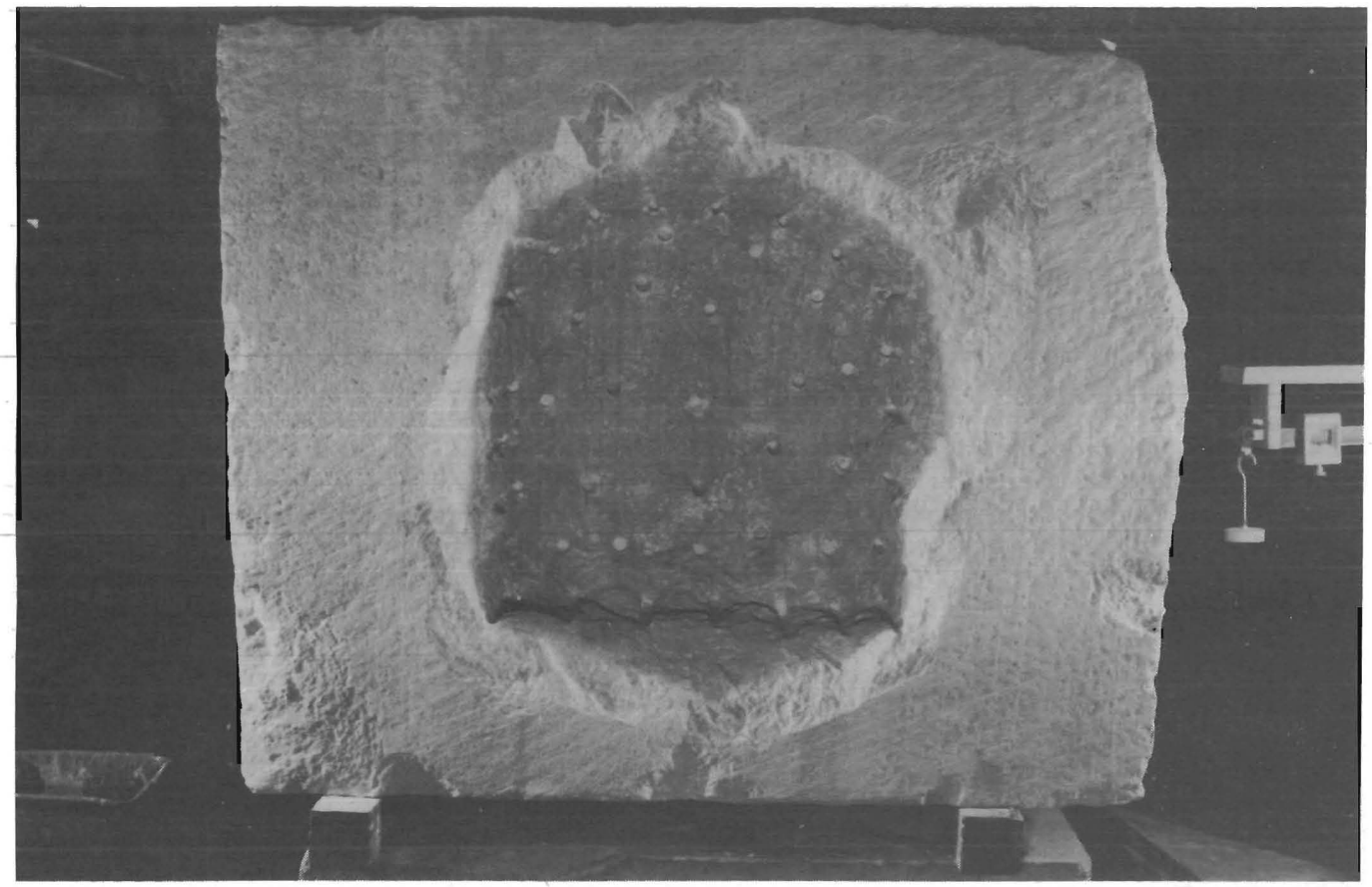

FIGURE 6.—Simulated drift in which breaks were made successively over previous breaks.

IN-HOLE COMPONENTS DESIGN OPTIMIZATION

To improve splitter performance, experiments with the tool's three in-hole components were conducted. The thrust-rod component operated independently of the wedge and feather and was a relatively simple piece to optimize. However, the wedge and feather components, which interact with one another and the rock, were mutually sensitive to design changes (fig. 7). In-hole components that varied in geometry and metallurgy were monitored in this program for their longevity and their influence on splitter performance.

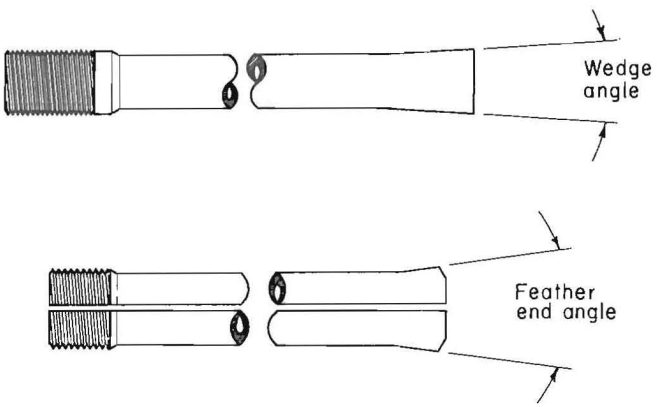

FIGURE 7.—Wedge (top) and feather (bottom) detail.

The thrust rod, which operates against the hole bottom and is loaded primarily in compression by this action, performed without fault. This component was made from an oil-hardening tool steel, American Iron and Steel Institute (AISI) Type 02, that was hardened to 60 Rockwell hardness C scale (R_c).

The geometry and metallurgy of the wedge have been varied with mixed success. The 7° wedge angle presently used is a compromise between increased wedge angle for quicker expansion of the feathers and decreased angle for increased mechanical advantage. In operation, the wedge is drawn back into the feathers. This action loads the wedge with a relatively small tensile stress and a much greater compressive stress where it contacts with the

feathers. The steel that the wedge is made from is the same AISI Type 02 that was used in the thrust rod. The wedge is hardened to about 56 R_c and does not show the wear or material creep of those made from lower strength steels, nor does it exhibit the brittle failure problems associated with wedges of greater hardness.

As failure of the feathers was the most persistent problem encountered with the in-hole components, project personnel experimented with a variety of steels to improve the performance of this component (table 2). Operation of the splitter subjects the feathers to extremes of tensile and compressive stresses and also puts them in contact with highly abrasive rock. This forced a compromise in metallurgy between high-strength hardened steels, which are prone to brittle failure, and lower strength steels, which are more ductile and thereby fail plastically or through wear. The most satisfactory alternative at present is a heat-treated, oil-hardening tool steel (AISI Type L6). This steel, which differs from that used for the wedge because of its increased toughness, is hardened to about 52 R_c and possesses enough ductility to greatly reduce the chance of brittle failure, yet it maintains sufficient strength to minimize material creep and wear.

Because of the radial-axial splitter's sensitivity to feather design, alternative feather geometrics were tested to determine their performance. Feathers with included end angles of 3°, 15°, and 30° were fabricated and tested in all three materials. Time and materials constraints reduced the number of tests conducted to a level below that which was desired, and additional testing should be carried out. However, the testing accomplished demonstrated that feather geometry influences splitter performance.

TABLE 2. - Steels used for wedge and feather components

Component	AISI type	Hardness, R_c	Failure mode	Trials to failure
Wedge....	420	40	Ductile.	10
	630	44	...do...	20
	02	62	Brittle.	20
Feather..	630	44	Ductile.	15
	02	52	Brittle.	8
	02	60	...do...	2

Increased feather end angle acts as a stress riser, effectively reducing the force required to produce fractures. However, the stress-riser benefit is not apparent in soft rocks. Owing to the low compressive strength of concrete, local crushing occurred at the feather-concrete interface when using 15°, and 30° feathers, negating the advantage of their increased end angles. More apparent is the positive effect of increased end angles when operating in granite. Here the 15° and 30° end-angle feathers caused a clear reduction in force requirements and permitted breaks to be made at greater depths. The 3° end-angle feathers performed with great difficulty in the granite at shallow depths and were incapable of producing breaks at depths exceeding 1.25 in; they were therefore excluded from further evaluation. The data from the 3° feather tests can be found in appendix tables A-1 to A-3. Little difference in performance has been seen between the 15° and 30° feathers at this time; however, performance differences are likely in stronger materials (figures 8-10).

Of important note is the effect of feather angle on break effectiveness (panel C of figures 8-10). Break effectiveness does not appear to be influenced by the feather angle when a break can be made. The different feathers produced the same characteristic fracture path in each of the three materials. The volume of break material excavated by this characteristic path can most easily be quantified in terms of the depth (length measured from the surface to the fracture point), and the diameter of the excavated mass at the surface. Typically, the ratio of this diameter to depth 7:1. A conservative approximation for the volume of the mass excavated can be made using this ratio and approximating the fracture path curve by a straight line (fig. 11). Assuming that a cross section of the fractured mass has a triangular shape,

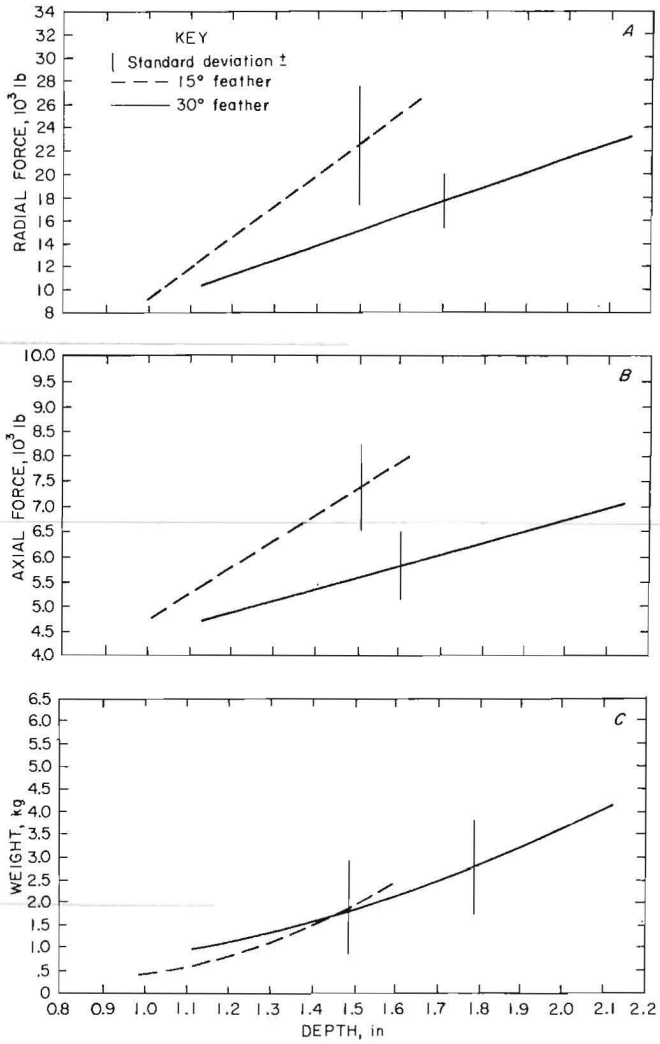

FIGURE 8.—Feather comparisons versus depth of (*A*) radial force, (*B*) axial force, and (*C*) weight of material removed in concrete.

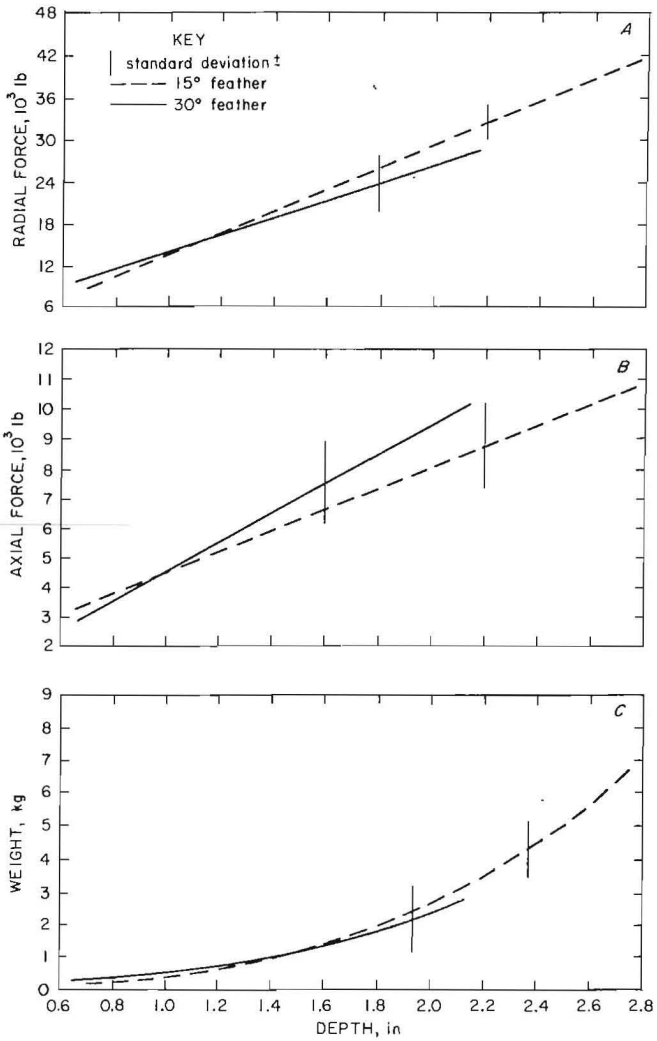

FIGURE 9.—Feather comparisons versus depth of (*A*) radial force, (*B*) axial force, and (*C*) weight of material removed in limestone.

with the base length equal to the depth and height equal to three and one-half times the base length, the volume can be approximated using a solid revolution method, as

$$V = (3.5^2)\ 1/3\ D^3$$

where D equals the depth.

However, as pointed out earlier, the 3° feathers were not capable of producing breaks in granite at extended depths. This is an important aspect in that a change in feather design alone, from 3° to 15° or 30°, allows the splitter to be successful in tougher rocks at greater depths.

The data from these tests are presented in graphical form in figures 8-10 and in tabular form in tables A-1 to A-3. (All radial and axial forces presented are peak loads and depths are measured from the surface to the fracture-initiation point.) The curves drawn in figures 8-10 relating the loads to the depth of break represent the best fitting linear regression equations. The remaining curves (figures 8*C*, 9*C*, and 10*C*) relating the break weight to the depth represent the best fitting power-curve regression equations. The best fitting regression equations, along with their corresponding coefficients of determination, are given in table A-4.

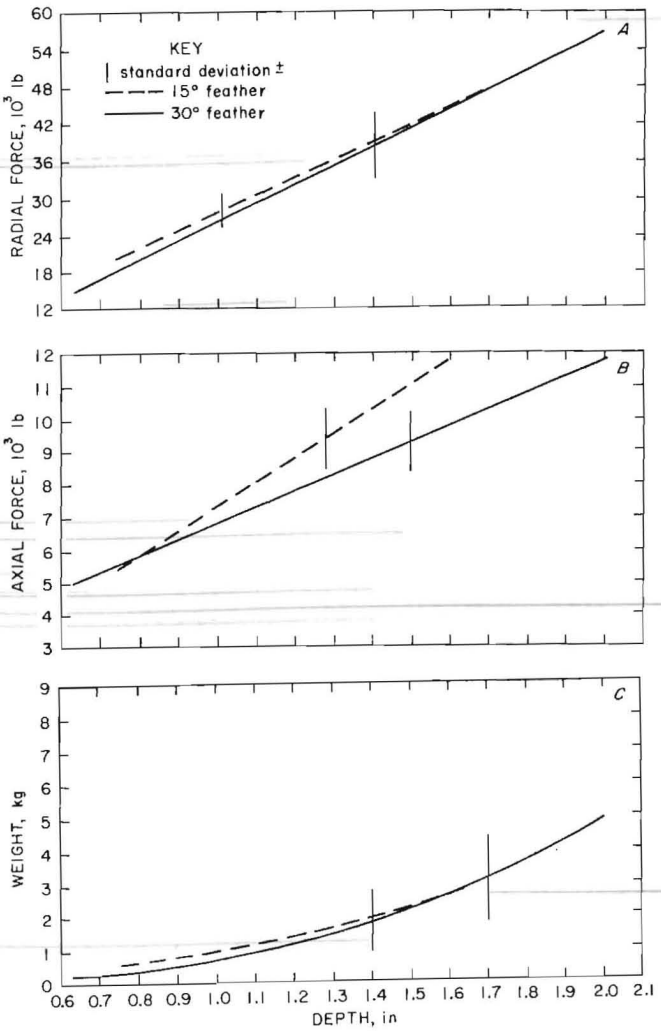

FIGURE 10.—Feather comparisons versus depth of (*A*) radial force, (*B*) axial force, and (*C*) weight of material removed in granite.

PARAMETRIC INVESTIGATIONS

Limestone and granite blocks were tested in this investigation for the relationships between (1) depth of break and radial- and axial-force requirements and (2) depth of break and break effectiveness. Break depth was varied from 0.625 through 2.75 in, and testing was conducted using 15° and 30° feathers, respectively, in the limestone and granite blocks. Data resulting from these tests are listed in tables A-5 and A-6.

The relationships between force parameters and depth of break were studied using linear regression-analysis

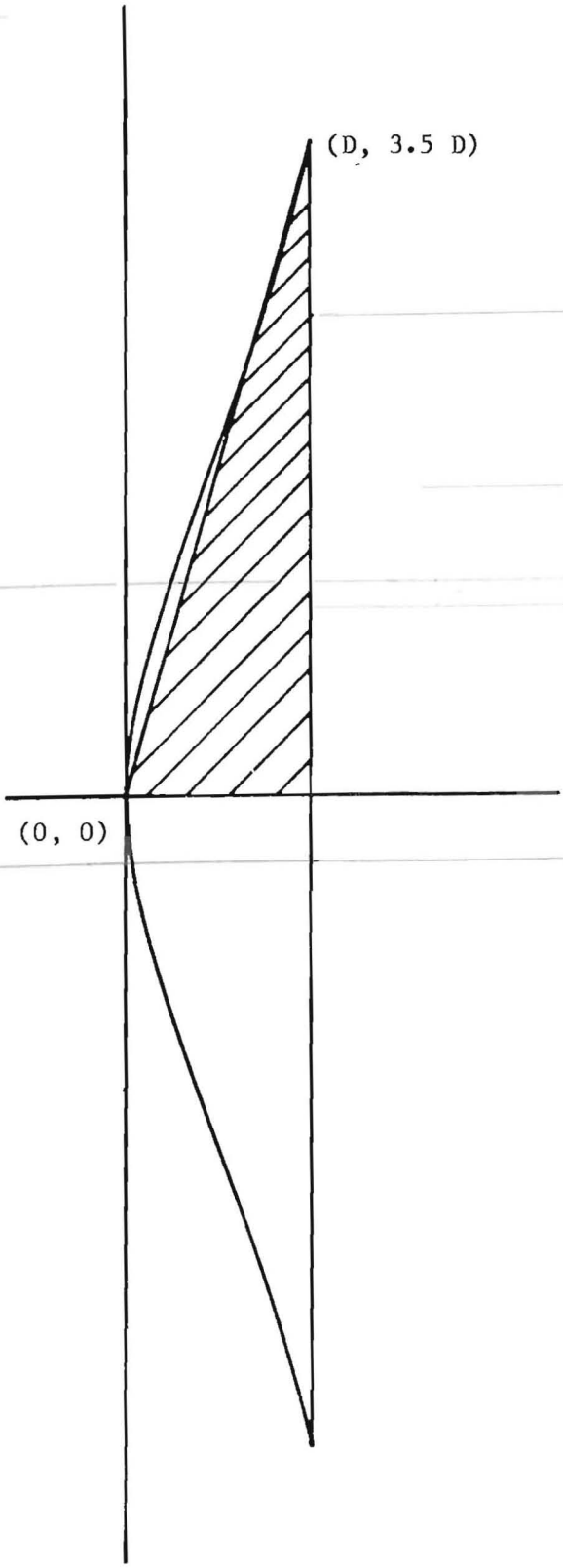

FIGURE 11.—Volume approximation.

techniques. These analyses resulted in the following functions and coefficients of determination (r^2).[3]

For limestone:

$$A = 3{,}380\ D + 1{,}272,\ r^2 = 0.54 \quad (1)$$

and $$R = 15{,}338\ D - 1{,}800,\ r^2 = 0.89 \quad (2)$$

For granite:

$$A = 5{,}079\ D + 1{,}755,\ r^2 = 0.82 \quad (3)$$

and $$R = 30{,}490\ D - 4{,}748,\ r^2 = 0.85 \quad (4)$$

where A = maximum axial force, lb,

R = maximum radial force, lb,

and D = depth of break, in.

Figures 12 and 13 show the data plots and regression curves that best fit these data. The good coefficients indicate that predictable radial-axial force loading combinations exist for these rocks. The one low coefficient that relates axial force to depth for experiments in limestone may be due to a variation in bed strength as the splitter was worked parallel with the bedding in several different beds. The radial-force coefficient might not have fluctuated as much because of its somewhat artificial nature, in that, during the course of testing, an experienced operator could set the initial radial load so that no slipping of the tool would occur. Therefore, the maximum radial load recorded would reflect this initial load, rather than a load applied in response to tool slippage. As a result, the recorded radial load was less dependent on individual bed strength and, at times, is a reflection of operator control. Figure 14 contrasts the forces required to produce breaks in limestone and granite. The positions of the curves are indicative of the relative resistance to fracturing by the two rock types.

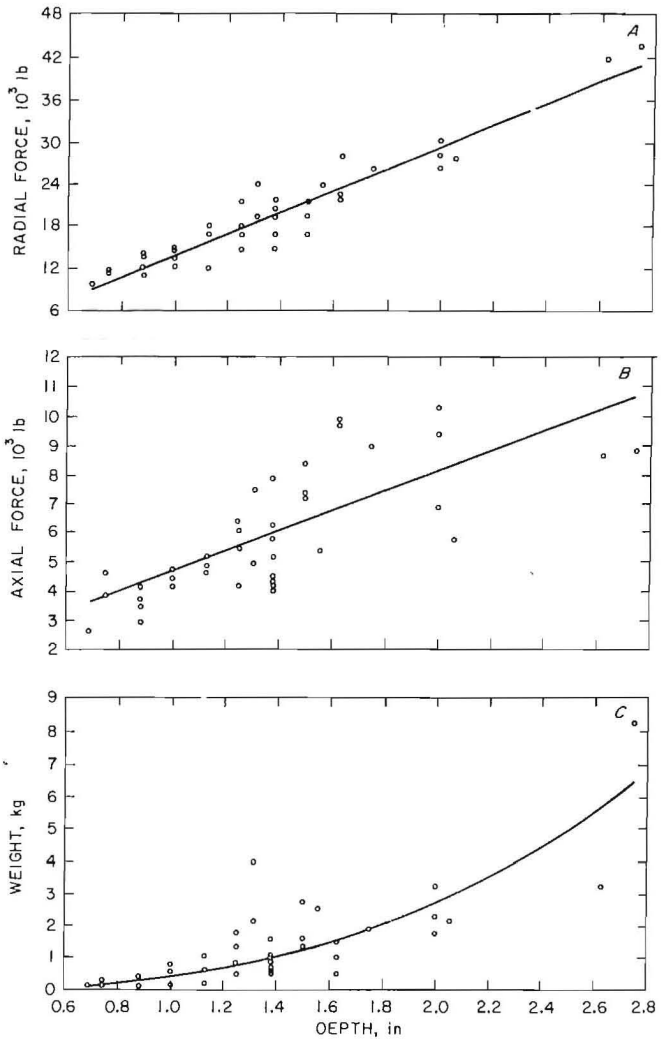

FIGURE 12.—Parametric comparisons versus depth of (*A*) radial force, (*B*) axial force, and (*C*) weight of material removed in limestone.

Break effectiveness was based on the quantity of material removed by each test. Regression analysis performed on this parameter, as it relates to break depth, resulted in the following function and coefficient of determination for limestone:

[3]Coefficient of determination is the proportionate reduction of total variation associated with the use of the independent variable. Thus, the larger the coefficient, the greater the total variation reduced by introducing the independent variable.

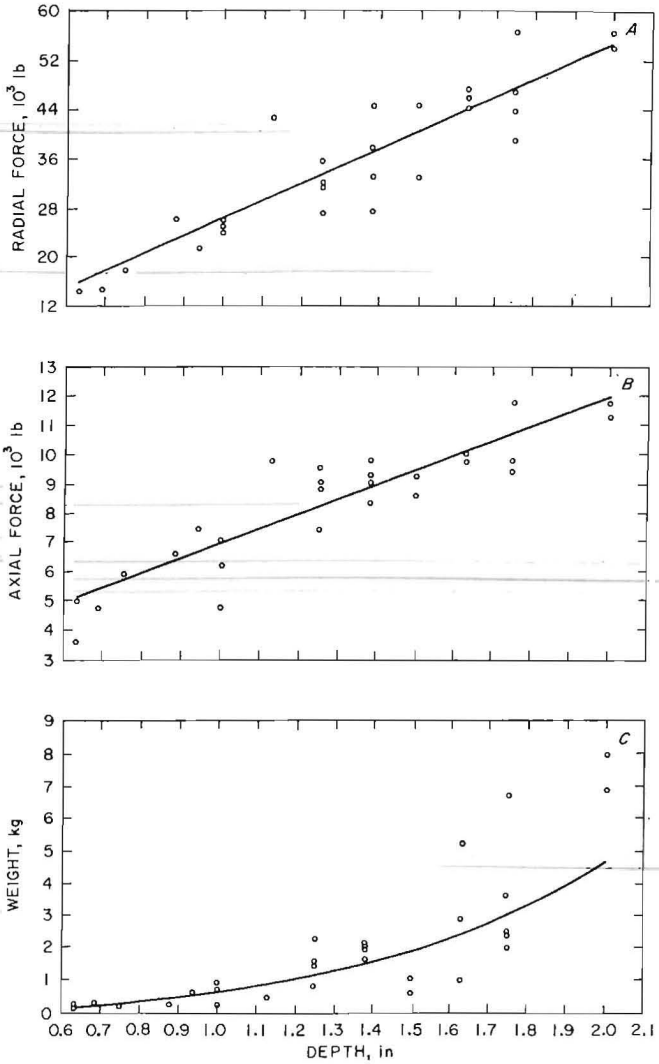

FIGURE 13.—Parametric comparisons versus depth of (*A*) radial force, (*B*) axial force, and (*C*) weight of material removed in granite.

$$W = 384\ D^{2.77},\ r^2 = 0.67, \qquad (5)$$

where W = quantity of material removed in grams.

Similarly, the function for granite is

$$W = 608\ D^{2.97},\ r^2 = 0.80. \qquad (6)$$

These empirical estimates of material removed agree well with the assumed relationship previously given where the volume, and thereby the weight of material removed, is proportional to the depth of break to the third power. The data plots and regression curves that best fit these data are shown in figures 12*C* and 13*C*.

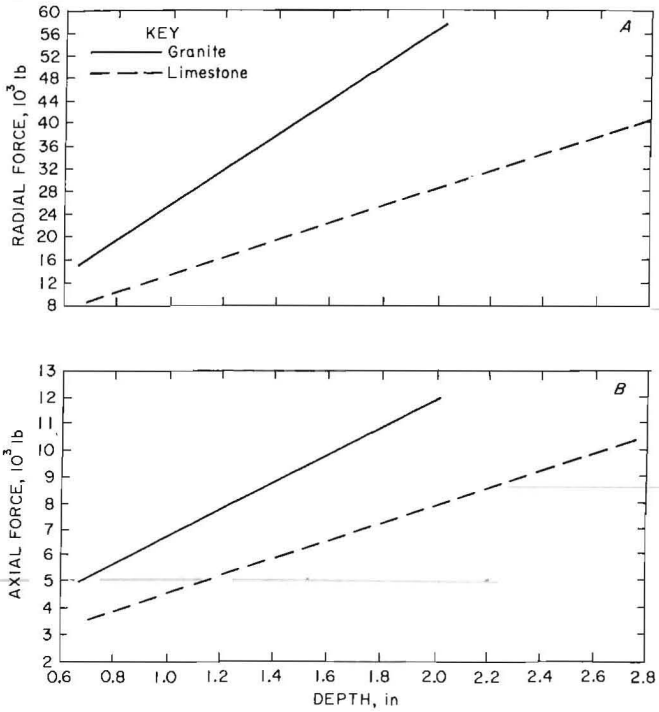

FIGURE 14.—Limestone and granite comparisons versus depth of (*A*) radial force and (*B*) axial force.

OPERATIONAL VARIABLES

Concerning the operational characterisics of the radial-axial loading splitter, investigations were made into the effects of breaking simultaneously with two splitters and of varying splitter orientation with the surface and rock structure. Optimization of splitter performance was pursued through efforts to minimize break forces and maximize the quantity of material removed by the break.

These investigations were made because of the effect that variation of confinement has on break geometry. Confinement involves the spatial orientation of the surface and discontinuities of the rock mass in which the break is to be made. Included in these categories are irregular face contour, nearness of an additional face or of an excavation's perimeter, natural discontinuities such as bedding planes or fractures that have not been recemented, and fractures that had begun, but were not completed by previous breaks. In general, increasing confinement increases the forces required to

produce a break. From the simulated drifting experiments in limestone, it was found that break effectiveness can be maintained through proper manipulation of the splitter, even in the great confinement present within the drift. Figure 15 represents the cumulative weight of material removed versus the number of breaks from the simulated drifting operation. Break effectiveness appears to fall off slightly with full confinement; however, the dramatic decrease in effectiveness reported previously by the Bureau (1) has been reduced through more efficient splitter manipulation. Data from the simulated drifting experiments can be found in table A-7.

Splitter Orientation

Splitter orientation is important because this mechanical excavation tool is directional with the loads it applies. The fracturing process will therefore become more efficient if the loads are applied to take advantage of any weaknesses presented by the rock or by the face contour. During the excavation of the simulated drift, a great deal of experience and understanding was gained concerning the effect of different break geometries on splitter performance.

There are three basic types of face contours that impose different confinement on the splitting operation and, thereby, result in different break geometries (fig. 16). The first (fig. 16*A*) is bordered by one or more additional free faces. The second (fig. 16*B*) is basically planar and infinite as far as the fracturing process is concerned, although it may have irregular contours, and the third (fig. 16*C*) is bordered by one or more confining walls. Each of these situations would be excavated differently to provide the greatest efficiency in the splitting operation.

Operators should take advantage of any additional free face as presented by the first situation, because it offers less confinement on the splitting process. Splitters can be operated near the edge in a slabbing-type operation under a predominantly radial load, or in their normal radial-axial fashion farther from the edge, but near enough so that the generated fracture will run to the additional free face rather than to the surface of the working face. When utilizing this technique, it appears

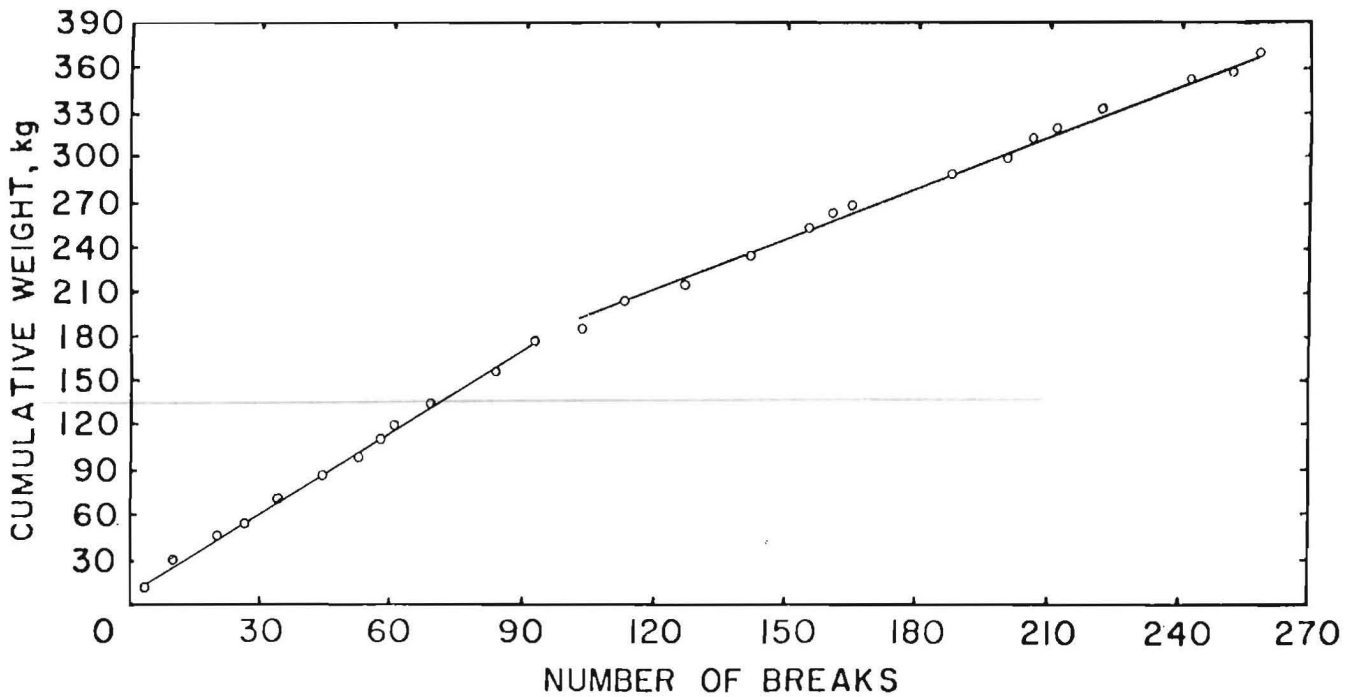

FIGURE 15.—Cumulative weight of material removed versus number of breaks, simulated drift.

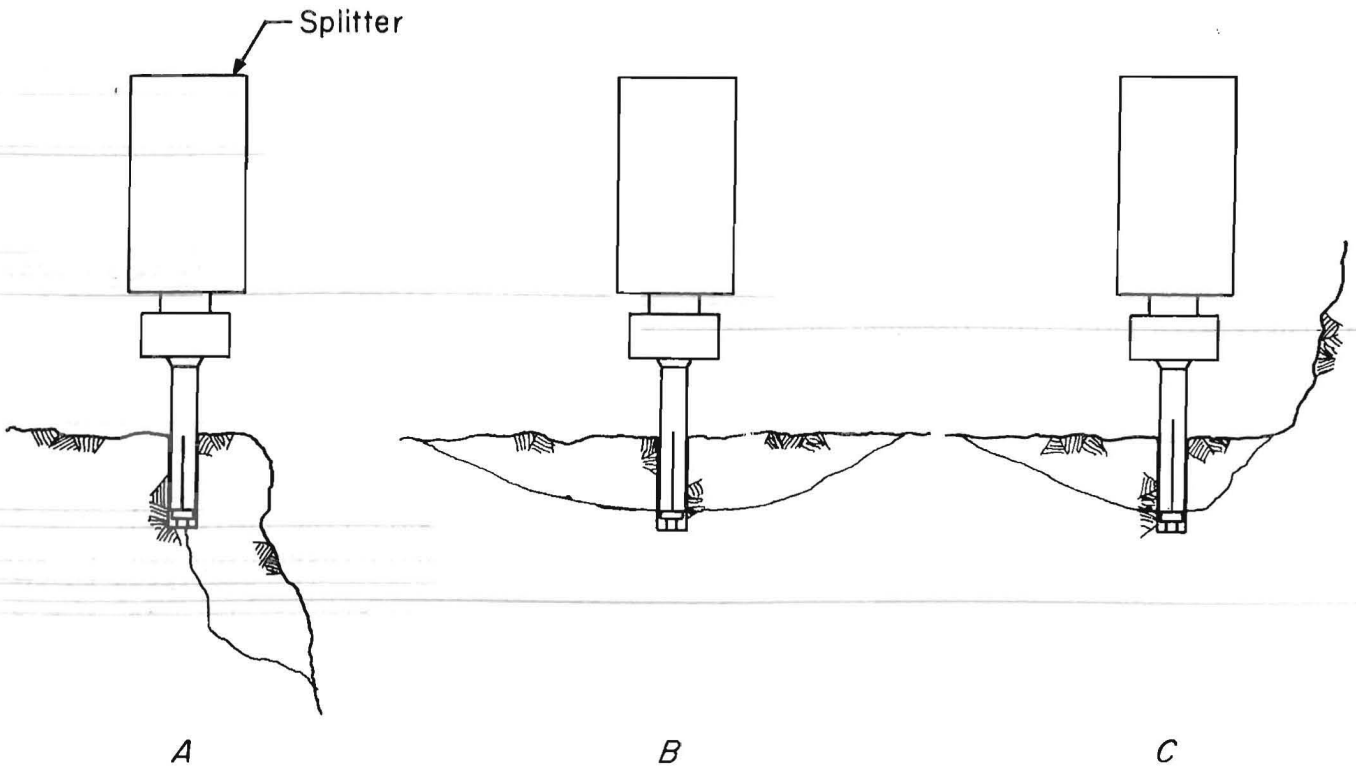

FIGURE 16.—Possible confinements on the splitting process. *A*, Bordered by a free face; *B*, planar; *C*, bordered by a confining wall.

that break forces remain the same but the quantity of material removed can be greatly increased. At times, depending on the distance to the edge, this technique requires radial forces greater than those required for a normal break at the same depth. However, the axial-force requirements will be much lower, if needed at all.

The planar face presented by the second situation would be best excavated by operating the splitter in its normal radial-axial loading fashion, producing the classic plug-type break geometry. The splitting operation may be performed and repeated singly, or with groups of splitters, to advance the face.

The third situation, which is similar to working near the wall of a heading, has proven to be the most difficult to excavate and should be avoided if possible. If splitters are worked in a confined area near the wall, fractures will be generated to the unconfined regions away from the bordering walls; however, these fractures will extend no farther than those without the confinement, and the break to the confined area will be minimal. This situation greatly reduces both the splitting and operational efficiencies. To alleviate this problem, the area away from the confinement should be excavated first. In the simulated drifting experiments, the problem of confinement was overcome when, a method of gauging was developed where the central portion of the face was advanced first, after which splitters in pairs were worked parallel to the advance, excavating the area near the wall with ease. This represents one method of meeting the problem without much loss in operational efficiency.

Equally important to the efficiency of splitting is the orientation of the splitter to the rock structure. Preliminary laboratory testing in bedded limestone has shown that the quantity of material removed by a break can be greatly increased when splitting along the bedding planes. Testing was conducted working in the same block of limestone with breaks generated along the bedding (tool working perpendicular) and

across the bedding (tool working parallel). When the tool was operated perpendicular to the bedding, sheets of material many times the normal break size were excavated. In these tests, fractures generated by the splitter would follow the bedding planes until sheets of material would snap free of the mass.

Paired Breaking

Paired breaking is the term used to describe tests in which a pair of splitters are operated together in close proximity to generate a single break. To ensure good interaction between the tools, the distance between them was kept proportional to their depth of operation. Spacing too close resulted in breaks that were only slightly larger than what a single tool could generate, and excessive spacing resulted in independent, distinct single breaks. Operating the splitters in this manner can reduce the forces required for producing breaks and may add to their effectiveness. Data from the paired-splitter testing program are listed in tables A-8 and A-9.

Figure 17 represents the force study of paired versus single breaks in limestone. It is apparent from the regression curves fitted to these data that breaking with a pair of splitters reduces the forces required. Similarily, figure 18 represents the force study of paired versus single breaks in granite. The regression curves fitted to these data indicate that the forces required are not affected by breaking with splitter pairs in granite. This is probably due to a lack of sufficient interaction of the stress fields produced by the individual splitters in the granite, as a result of the granite's higher strength.

Figure 17*C* represents the comparisons of material removed by the two break conditions when operating in limestone. Because there are two splitters working in the paired-break tests, the weights presented for the paired breaks are half of the actual weight removed for a better comparison with the single-break data. An increase in effectiveness was expected

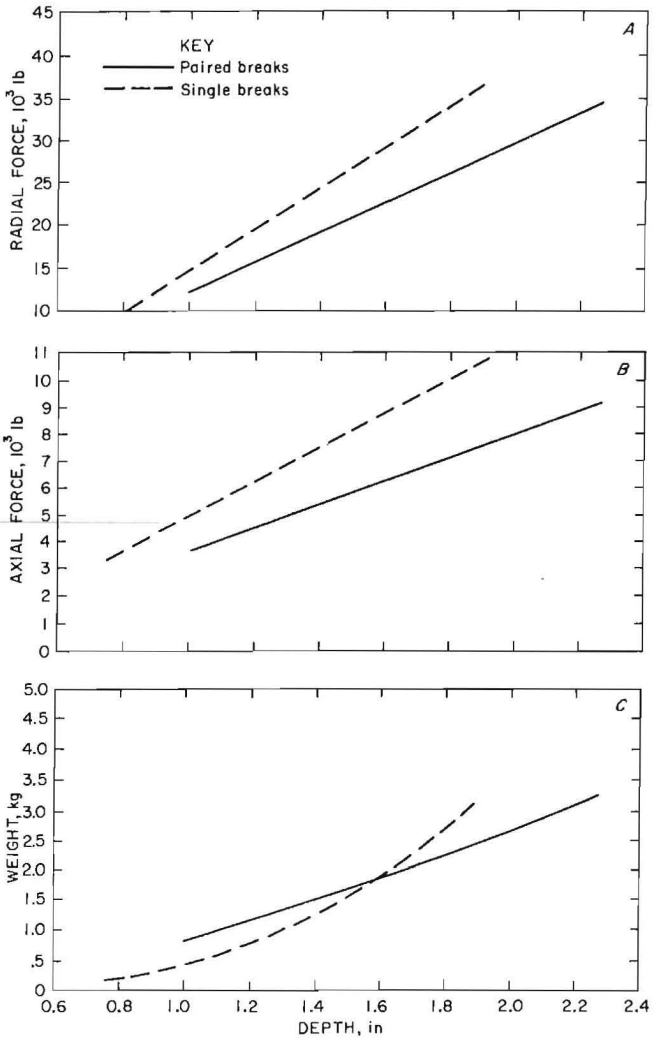

FIGURE 17.—Paired- versus single-break comparisons versus depth of (*A*) radial force, (*B*) axial force, and (*C*) weight of material removed in limestone.

when breaking with splitter pairs; however, the data show no difference. Figure 18*C* shows a similar comparison when operating in granite. Again, no change in effectiveness can be seen when operating the splitters singly or in pairs. (See table A-4.)

The technique of paired breaks proved effective when working the gauge of the simulated limestone drift. This operation was accomplished by driving the interior of the drift's face first, which opened an additional surface for the splitters to break toward, then operating the splitter pair in gauge holes that were nearly parallel to the direction of the drift's advance. Most breaks made were under radial load alone; however, if

splitter limits of capability were reached, follow-up axial loading was used to generate the break. This technique proved very effective in excavating and maintaining the drifts gauge.

DRILL-SPLIT CONCEPT POTENTIAL

The drill-split excavation concept has potential as an alternative to the drill-blast method used in the development and production activities of underground mining. The concept parallels conventional blasting techniques in that both use drilling to gain access to the rock, and both can operate in a broad range of rock types. However, the similarity in drill-split and drill-blast technologies ends here.

The health and safety advantages of splitting technology, stated in the introduction, are supplemented by the radial-axial loading splitter's design and operational characteristics. Foremost may be the self-contained nature of this mechanical excavation tool; it does not require a mass or additional systems to react its excavation forces. This makes the tool versatile, giving it the ability to go anywhere a drill can. Perhaps more importantly, it allows the tool the same flexibility as drill-blast systems, enabling it to excavate in any orientation, to create an opening of any shape, and to take advantage of the weaknesses inherent in host-rock formations. An additional factor of the tool's versatility is that it is scalable. Our work with splitters leads us to the assumption that commercial-size tools can be built and used to generate as large a break as required. This enables the tool to operate efficiently when excavating in a range of settings, creating from very small to large openings.

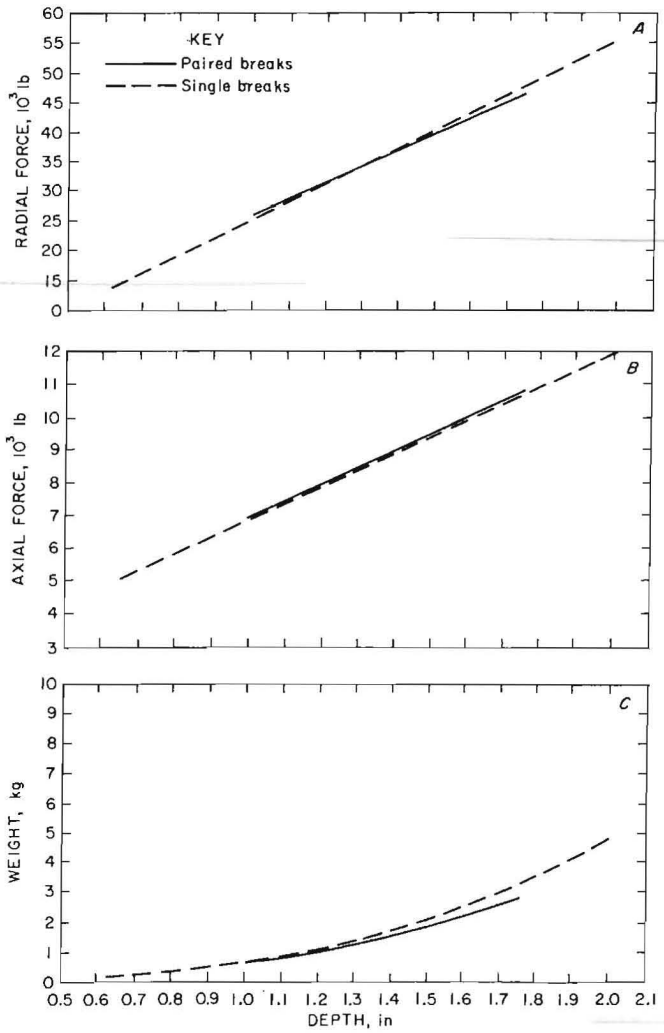

FIGURE 18.—Paired- versus single-break comparisons versus depth of (*A*) radial force, (*B*) axial force, and (*C*) weight of material removed in granite.

The operational characteristics of the splitter are also attractive. The tool is easy to operate and requires little operator skill, and in most cases a single operator should be able to handle both the drilling and splitting operations. The excavation process is an uncomplicated repetition of the drill-split cycle, which requires a short time interval. This continuous-excavation technique is nondisruptive to nearby mining activities, unlike the involved activities in preparing and firing a blast.

There is widespread potential for application in underground mining because of the splitter's ability to excavate development openings. Furthermore, the tool's versatility permits these openings to be vertical or inclined shafts, or drifts of any size or shape.

Of the major underground mining methods, only in caving, long-hole, and sublevel stoping does the potential for

splitting appear as limited as production techniques. The remainder of the production methods including the steeply pitching seam (such as shrinkage, overhand, and underhand stoping), cut-and-fill, room-and-pillar, and open stoping are amenable to excavation by splitting.

FULL-SCALE DEVELOPMENT

The sucess of the reduced-scale splitters has led to the design and fabrication of a full-scale splitter and tool positioner (fig. 19). This splitter maintains the simplicity of the earlier designs and operates in the same manner. The tool positioner carries the splitter and a complementary drill, and in operation it places the splitter into the hole just finished by the drill.

The in-hole components for this splitter are designed to work within a predrilled hole of 0.625-in-diam, and to a depth of 14 in. These components are made of a tough, oil-hardening, tool steel that has performed well in the laboratory. The anticipated range of breaking depths run from 4 to 12 in, and these in-hole components require 2.50 in of overdrilling.

The splitter's hydraulic cylinder is made from high-strength aluminum and weighs just 50 lb. It has a 5.50-in diam bore and an operating pressure range of 0 to 3,000 psi. The full-scale splitter can provide maximum forces of 71,250 lb

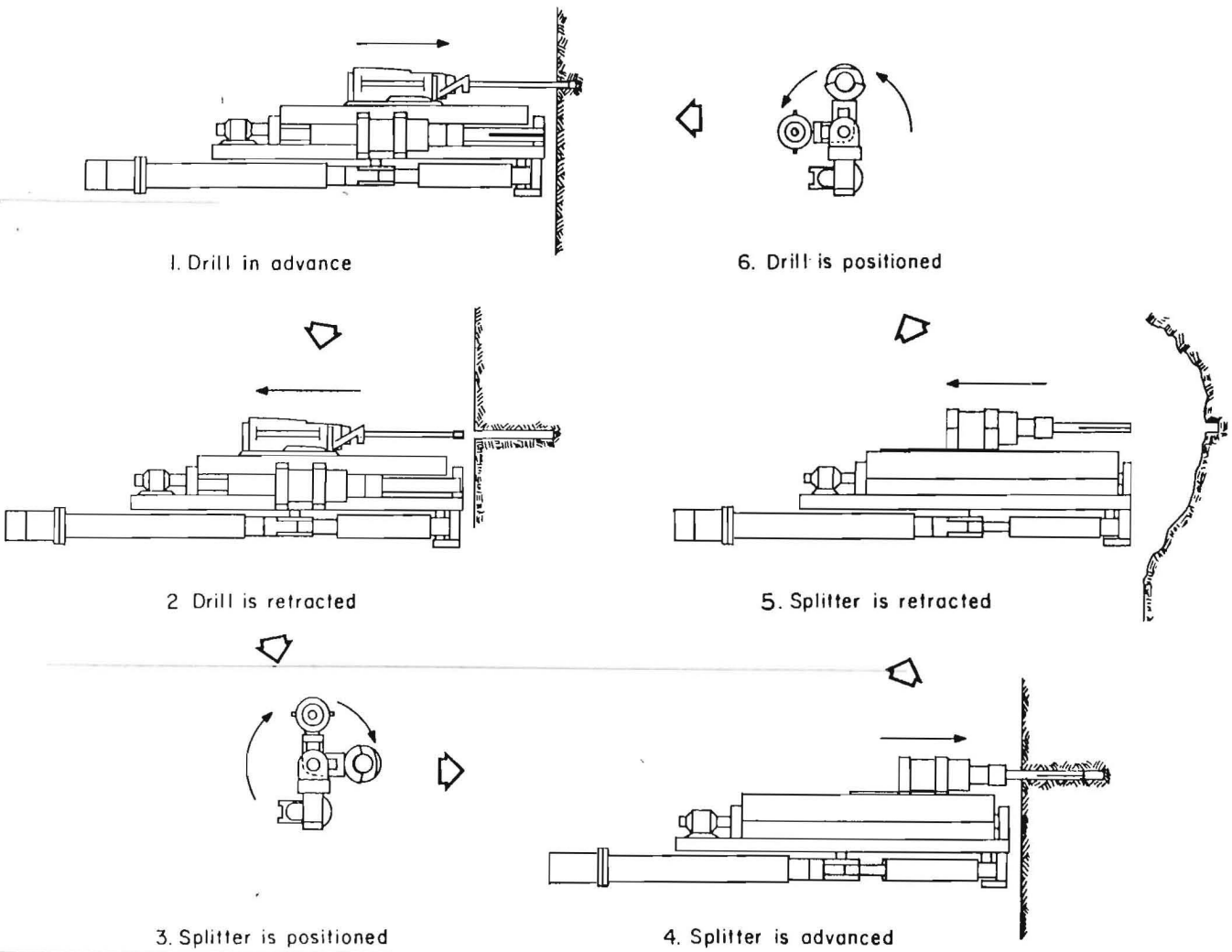

FIGURE 19.—Use of tool positioner to alternate drill and splitter operation.

axially and 345,000 lb radially, which is approximately six times the capability of the splitters used in this investigation.

The tool positioner is the Bureau's initial attempt to automate the drill-split process. It functions as a platform that will orient the tools with the face, advance and retract the drill, and then align and advance the splitter into the just-completed drill hole. Its design parallels that of a drill boom and feed, and it provides roll and swing operations as well as the tool alignment or indexing functions.

The full-scale unit will be used to determine if the splitter is capable of larger scale excavation, and to clarify the requirements for the positioner and the usefulness of an integrated drilling and splitting tool.

CONCLUSIONS

The metallurgical properties of the in-hole components are critical for satisfactory performance and working life of the splitting tool. The current components perform well; however, further testing is required to determine their working life.

Increasing the included end angle of the feathers creates a stress riser that influences splitter performance. The larger feather and angles definitely improved splitter performance when operating in granite; however, the effect can be compromised by crushing in weaker rocks. Because of this compromising effect, feather geometry should be investigated further to fully test its effect on performance. The good correlations generated between the forces required and depth of break indicate that preliminary testing in any rock should yield reliable equations with which predictions of force and tool requirements can be made.

Break geometry has been consistent throughout all materials tested. This indicates that splitter performance could be predictable in most rock types.

Breaking simultaneously appears to provide advantages in Kasota limestone. Decreases in required forces were observed when operating splitters simultaneously in limestone. However, no differences were found for similar operations in granite. The material property that governs interaction between the pair of splitters needs to be defined before the influence that breaking simultaneously will have on splitter excavation can be predicted.

The efficiency of splitting is significantly affected by the tool's orientation with the surface contours and the discontinuities in the rock.

The potential for drill-split excavation with radial-axial loading splitters is good. However, further investigations into tool-rock interactions should be undertaken to provide a better understanding of this relationship.

REFERENCES

1. Anderson, S. J., and D. E. Swanson. Laboratory Testing of a Radial-Axial Loading Splitting Tool. BuMines RI 8722, 1982, 26 pp.

2. Cooper, G. A., J. Berlie, and A. Merminod. A Novel Concept for Rock-Breaking Machine, Part II, Excavation Techniques and Experiments at Large Scale. J. Proc. R. Soc. Lond., Ser. A, v. 373, No. 1754, 1980, pp. 352-372.

3. Kaplan, M., and D. Chazin. Potential Applications of Drill-Split Fragmentation Systems in Underground Mines (contract J0285016, Sci. Appl., Inc.). BuMines OFR 86-80, 1979, 188 pp; NTIS PB80-210792.

4. Rhyming, I., G. A. Cooper, and J. Berlie. A Novel Concept for Rock-Breaking Machine, Part I, Theoretical Consideration and Model Experiments. J. Proc. R. Soc. Lond., Ser. A., v. 373, No. 1754, 1980, pp. 331-351.

5. Unger, H. F., and R. R. Fumanti. Percussive Drilling With Independent Rotation. BuMines RI 7692, 1972, 21 pp.

6. Chatterjee, S., and B. Price. Regression Analysis by Example. J. Wiley, 1977, 228 pp.

APPENDIX

TABLE A-1. - Feather-comparison data for concrete

Break number	Feather angle, °	Depth of break, in	Weight of break material, g	Force, lb	
				Radial	Axial
1.....	3	1.50	3,642	16,150	5,978
2.....	3	1.50	2,256	16,625	6,566
3.....	3	1.25	1,007	17,100	5,390
4.....	3	1.63	1,686	22,562	9,800
5.....	3	2.00	6,139	21,375	9,457
6.....	3	1.63	2,147	21,375	8,820
7.....	3	1.38	1,555	14,250	6,125
8.....	3	1.38	2,070	11,875	6,909
9.....	3	1.13	1,779	16,625	5,047
10.....	15	1.00	288	14,250	5,880
11.....	15	1.50	1,329	30,281	8,820
12.....	15	1.63	2,408	28,975	7,595
13.....	15	1.63	1,869	28,500	9,065
14.....	15	1.25	546	16,625	5,733
15.....	15	1.25	224	14,250	6,027
16.....	15	1.50	4,380	14,250	6,860
17.....	15	1.25	1,624	14,250	5,243
18.....	15	1.25	1,161	11,875	5,586
19.....	30	1.38	1,791	14,250	5,390
20.....	30	1.38	2,671	11,875	5,145
21.....	30	1.13	1,109	9,500	4,998
22.....	30	1.38	3,511	11,875	4,655
23.....	30	2.00	3,035	20,187	5,880
24.....	30	2.00	4,890	21,375	6,517
25.....	30	1.75	1,793	21,375	5,292
26.....	30	1.75	1,196	22,562	6,811
27.....	30	2.13	6,008	20,425	8,330
28.....	30	1.63	1,371	21,375	5,684
29.....	30	1.13	381	10,687	4,655
30.....	30	1.38	1,677	10,687	4,900
31.....	30	1.38	1,143	14,250	6,174
32.....	30	1.38	1,328	14,250	6,615

TABLE A-2. - Feather-comparison data for limestone

Break number	Feather angle, °	Depth of break, in	Weight of break material, g	Force, lb	
				Radial	Axial
1.....	3	1.50	360	17,812	7,840
2.....	3	1.50	754	28,500	7,350
3.....	3	1.25	401	17,812	5,145
4.....	3	1.38	1,142	26,125	5,390
5.....	30	1.50	1,759	14,250	5,390
6.....	30	1.50	3,151	19,000	8,330
7.....	30	1.38	831	16,625	7,742
8.....	30	1.25	282	13,062	6,492
9.....	30	1.63	282	17,812	8,134
10.....	30	.88	190	16,625	3,038
11.....	30	1.00	420	22,562	6,664
12.....	30	1.63	995	22,562	10,045
13.....	30	1.63	527	35,625	9,800
14.....	30	1.00	468	14,250	3,920
15.....	30	1.25	881	20,187	7,840
16.....	30	1.75	2,613	23,750	8,820
17.....	30	1.19	819	15,437	5,880
18.....	30	.94	383	14,250	4,165
19.....	30	1.63	4,870	21,375	8,575
20.....	30	1.50	960	17,812	7,227
21.....	30	.94	672	11,875	3,430
22.....	30	.63	130	8,312	2,450
23.....	30	1.00	337	14,843	3,062
24.....	30	1.81	3,840	22,562	8,379
25.....	30	2.00	1,464	27,312	9,187
26.....	30	2.13	3,086	29,687	8,575
27.....	30	1.06	934	13,062	3,430
28.....	30	1.50	1,354	15,200	4,459
29.....	30	1.25	912	16,625	3,626
30.....	30	.88	887	10,687	3,381

NOTE.--The 15° feather-angle data are shown in table A-4.

TABLE A-3. - Feather-comparison data for granite

Break number	Feather angle, °	Depth of break, in	Weight of break material, g	Force, lb	
				Radial	Axial
1.....	3	0.75	234	42,750	10,290
2.....	3	1.00	384	35,625	7,350
3.....	3	1.00	1,180	47,500	8,575
4.....	3	1.00	1,903	47,500	10,290
5.....	3	1.13	245	33,250	9,800
6.....	3	1.25	443	35,625	7,203
7.....	15	.75	189	19,000	5,537
8.....	15	.88	1,729	28,500	6,125
9.....	15	1.00	511	28,500	5,537
10.....	15	1.00	834	21,375	7,105
11.....	15	1.00	1,274	24,937	8,820
12.....	15	1.00	798	22,800	7,644
13.....	15	1.25	2,202	38,000	9,800
14.....	15	1.25	1,056	33,250	9,555
15.....	15	1.25	2,193	35,625	8,624
16.....	15	1.25	496	36,812	10,290
17.....	15	1.50	4,028	39,187	10,290
18.....	15	1.63	1,386	44,531	11,760

NOTE.--The 30° feather-angle data are shown in table A-5.

TABLE A-4. - Regression formulations

(R = radial force, lb; A = axial force, lb; D = depth, in; W = weight, g)

Figure description		Best fitting equation	Coefficient of determination, r^2	Figure description		Best fitting equation	Coefficient of determination, r^2
No.	Key			No.	Key		
FEATHER COMPARISON				PAIRED-VERSUS SINGLE-BREAK COMPARISON			
8*A*	15°	R = 27,462 D - 18,159	0.59	17*A*	Paired	R = 18,256 D - 6,389	0.82
	30°	R = 13,184 D - 4,481	.76		Single	R = 24,652 D - 9,773	.81
8*B*	15°	A = 5,391 D - 587	.65	17*B*	Paired	A = 4,474 D - 825	.82
	30°	A = 2,263 D + 2,265	.51		Single	A = 6,402 D - 1,338	.81
8*C*	15°	$W = 268\ D^{4.62}$	.57	17*C*	Paired	$W = 858\ D^{1.63}$	.41
	30°	$W = 647\ D^{2.46}$	.50		Single	$W = 414\ D^{3.20}$	.60
9*A*	15°	R = 15,338 D - 1,800	.89	18*A*	Paired	R = 27,395 D - 858	.89
	30°	R = 12,199 D + 1,925	.57		Single	R = 30,490 D - 4,748	.85
9*B*	15°	A = 3,380 D + 1,272	.54	18*B*	Paired	A = 5,258 D + 1,658	.72
	30°	A = 5,380 D - 981	.69		Single	A = 5,079 D + 1,755	.82
9*C*	15°	$W = 384\ D^{2.77}$	.67	18*C*	Paired	$W = 624\ D^{2.71}$	.41
	30°	$W = 477\ D^{2.27}$	.52		Single	$W = 608\ D^{2.97}$	.80
10*A*	15°	R = 29,013 D - 2,225	.85				
	30°	R = 30,490 D - 4,748	.85				
10*B*	15°	A = 7,232 D + 131	.82				
	30°	A = 5,079 D + 1,755	.82				
10*C*	15°	$W = 813\ D^{2.32}$	.39				
	30°	$W = 608\ D^{2.97}$	.80				

TABLE A-5. - Parametric-investigation data for limestone

Break number	Feather angle, °	Depth of break, in	Weight of break material, g	Force, lb	
				Radial	Axial
1.....	15	1.13	1,039	16,625	4,606
2.....	15	1.25	1,795	21,375	4,165
3.....	15	1.00	577	14,250	4,410
4.....	15	1.50	2,729	21,375	8,330
5.....	15	1.75	1,942	26,125	8,967
6.....	15	.88	108	13,062	2,940
7.....	15	1.00	137	13,062	4,165
8.....	15	.88	410	13,300	4,165
9.....	15	1.00	681	13,775	4,165
10.....	15	.75	246	10,687	4,655
11.....	15	.69	94	9,500	2,695
12.....	15	1.56	2,509	23,750	5,292
13.....	15	2.00	3,175	28,025	9,359
14.....	15	2.00	2,246	29,687	6,762
15.....	15	1.38	561	20,425	7,840
16.....	15	1.63	1,012	28,025	9,653
17.....	15	.88	117	11,875	3,773
18.....	15	.75	201	11,162	3,895
19.....	15	1.50	1,570	19,000	7,105
20.....	15	.88	414	10,925	3,479
21.....	15	1.00	135	11,875	4,753
22.....	15	1.13	230	11,875	5,145
23.....	15	2.00	1,740	26,125	10,167
24.....	15	1.25	1,365	14,250	5,390
25.....	15	1.38	656	14,250	6,125
26.....	15	1.38	1,539	19,000	4,459
27.....	15	1.38	1,086	16,625	4,287
28.....	15	1.31	2,153	23,750	4,900
29.....	15	1.31	3,959	19,000	7,448
30.....	15	1.38	843	19,000	4,018
31.....	15	1.38	987	14,250	4,165
32.....	15	1.25	844	17,812	6,002
33.....	15	1.38	490	21,375	5,733
34.....	15	1.38	603	21,375	5,145
35.....	15	2.06	2,154	27,312	5,635
36.....	15	2.63	3,162	40,850	8,575
37.....	15	2.75	8,270	42,750	8,673
38.....	15	1.50	1,297	16,625	7,301
39.....	15	1.25	424	16,625	6,370
40.....	15	1.13	614	17,812	4,851
41.....	15	1.63	1,471	22,562	9,800
42.....	15	1.63	485	21,375	9,800

TABLE A-6. - Parametric-investigation data for granite

Break number	Feather angle, °	Depth of break, in	Weight of break material, g	Force, lb	
				Radial	Axial
1.....	30	1.38	1,684	27,550	8,330
2.....	30	1.50	1,144	33,250	8,575
3.....	30	1.25	1,461	33.250	9,555
4.....	30	1.75	3,715	47,500	9,800
5.....	30	1.00	620	23,750	6,982
6.....	30	.94	539	21,375	7,399
7.....	30	1.00	937	26,125	6,125
8.....	30	1.25	2,310	27,312	9,065
9.....	30	1.38	2,196	45.125	9,800
10.....	30	.88	243	26,125	6,517
11.....	30	.63	196	14,250	3,528
12.....	30	.75	213	17,812	5,880
13.....	30	1.00	294	24,937	4,655
14.....	30	1.63	5,349	47,500	9,800
15.....	30	2.00	7,028	54,625	11,270
16.....	30	1.75	2,497	39,187	9,432
17.....	30	1.25	831	35,625	8,820
18.....	30	1.75	2,017	57,000	11,760
19.....	30	.69	354	14,250	4,655
20.....	30	.63	164	14,250	4,900
21.....	30	2.00	8,052	57,000	11,760
22.....	30	1.63	1,075	46,312	10,045
23.....	30	1.38	1,930	38,000	9,065
24.....	30	1.25	1,585	32,062	7,350
25.....	30	1.13	480	42,750	9,800
26.....	30	1.75	6,780	57,000	11,760
27.....	30	1.50	606	45,125	9,310
28.....	30	1.63	2,958	45,125	9,800
29.....	30	1.75	2,344	43,937	9,800
30.....	30	1.38	2.095	33,250	9.310

TABLE A-7. - Data for simulated drift in limestone

Break number	Feather angle, °	Depth of break, in	Weight of break material, kg	Force, lb	
				Radial	Axial
1.....	15	2.25	9.1	47,500	10,290
2.....	15	1.88		40,375	9,555
3.....	15	1.63		28,500	6,860
4.....	15	1.75		28,500	8,820
5.....	3	1.75	23.2	36,812	9,065
6.....	3	1.88		39,187	9,800
7.....	3	.80		33,250	7,840
8.....	3	2.13		28,500	8,330
9.....	3	2.13		34,437	8,820
10.....	3	1.75		39,187	9,800
11.....	3	1.88		35,625	9,310
12.....	3	1.88	14.1	34,437	9,432
13.....	3	2.25		40,375	8,330
14.....	3	2.25		43,225	8,918
15.....	3	1.75		36,812	8,575
16.....	3	2.00		40,375	9,800
17.....	3	1.88		40,375	9,702
18.....	3	1.88		52,250	11,760
19.....	3	2.00		57,000	11,760
20.....	3	1.63		33,487	8,942
21.....	3	1.50	8.6	28,500	8,085
22.....	15	2.50		28,500	5,880
23.....	15	2.06		28,500	4,410
24.....	15	2.00		26,125	5,390
25.....	15	1.25		22,562	6,860
26.....	15	2.00		22,562	7,350
27.....	3	1.75		21,375	6,860
28.....	3	2.25	16.4	40,375	9,800
29.....	3	2.25		28,500	7,350
30.....	3	2.19		35,625	9,800
31.....	3	3.00		28,500	5,880
32.....	3	3.00		28,500	5,880
33.....	3	3.00		28,500	5,145
34.....	3	3.00		28,500	5,145
35.....	3	2.00	15.9	21,375	4,410
36.....	3	2.00		35,625	9,310
37.....	3	2.00		33,250	8,820
38.....	3	2.00		39,187	9,555
39.....	3	2.00		32,062	7,350
40.....	3	2.00		32,062	8,820
41.....	3	3.00		57,000	11,760
42.....	3	1.50		28,500	6,370
43.....	3	2.00		40,375	10,290
44.....	3	2.00		28,500	8,085
45.....	3	2.00		33,250	8,330

TABLE A-7. - Data for simulated drift in limestone--Continued

Break number	Feather angle, °	Depth of break, in	Weight of break material, kg	Force, lb	
				Radial	Axial
46.....	3	2.00		33,250	8,575
47.....	3	2.00		28,500	7,595
48.....	3	2.50		28,500	0
49.....	3	2.50	12.7	28,500	0
50.....	3	2.00		26,125	3,430
51.....	3	2.50		28,500	4,410
52.....	3	2.50		28,500	4,410
53.....	3	3.00		26,125	0
54.....	3	3.00		26,125	0
55.....	3	2.00	11.4	40,375	8,820
56.....	3	3.00		28,500	8,330
57.....	3	3.00		28,500	8,330
58.....	15	2.00		21,375	5,145
59.....	15	1.50	9.5	21,375	0
60.....	15	2.00		21,375	7,227
61.....	15	2.00		21,375	6,737
62.....	15	2.13		19,000	0
63.....	15	1.50		26,125	7,350
64.....	15	2.00		21,375	4,900
65.....	15	2.00	15.0	21,375	7,962
66.....	15	1.00		17,218	6,002
67.....	15	2.00		47,500	9,800
68.....	15	2.00		19,000	0
69.....	15	1.25		42,750	7,350
70.....	15	2.00		35,031	8,330
71.....	15	1.50		28,500	5,880
72.....	15	2.50		28,500	5,145
73.....	15	2.13		35,625	10,290
74.....	15	1.50		17,812	0
75.....	15	1.00		33,250	8,330
76.....	15	1.00	19.5	20,187	0
77.....	15	2.00		32,062	9,065
78.....	15	2.00		35,625	9,310
79.....	15	2.00		24,937	8,330
80.....	15	1.50		40,375	9,310
81.....	15	1.38		33,250	9,310
82.....	15	1.00		11,875	0
83.....	15	1.00		19,000	6,370
84.....	3	2.50		39,187	8,820
85.....	3	2.50		39,187	8,820
86.....	3	3.25		42,750	8,820
87.....	3	3.25		42,750	8,820
88.....	3	1.00	20.5	35,625	0
89.....	3	2.00		42,750	8,820
90.....	3	2.50		35,625	0
91.....	3	2.50		47,500	4,900
92.....	3	2.00		42,750	0
93.....	3	3.00		47,500	0

TABLE A-7. - Data for simulated drift in limestone--Continued

Break number	Feather angle, °	Depth of break, in	Weight of break material, kg	Force, lb	
				Radial	Axial
94.....	3	2.00		35,625	0
95.....	3	3.00		47,500	7,840
96.....	3	2.00		35,625	7,840
97.....	3	2.00		35,625	0
98.....	3	1.50		32,062	0
99.....	3	3.50	10.0	38,000	0
100.....	3	3.25		38,000	0
101.....	3	1.75		29,687	0
102.....	3	1.50		21,375	0
103.....	3	2.00		33,250	0
104.....	30	2.00		36,812	9,800
105.....	30	2.00		30,875	6,370
106.....	30	2.00		45,125	9,800
107.....	30	2.00		39,187	0
108.....	30	2.00		29,687	0
109.....	30	2.00	16.8	33,250	6,860
110.....	30	2.00		29,687	8,820
111.....	15	2.00		24,937	0
112.....	15	2.00		33,250	9,800
113.....	3	2.00		46,312	10,290
114.....	3	1.75		35,625	7,350
115.....	3	2.00		38,000	9,800
116.....	3	2.00		45,718	10,290
117.....	3	2.00		21,375	0
118.....	3	2.00		30,875	0
119.....	3	1.38		16,625	0
120.....	3	1.38		29,687	0
121.....	3	2.00	14.1	35,625	8,330
122.....	3	1.50		24,937	0
123.....	3	3.00		47,500	7,840
124.....	3	2.00		33,250	0
125.....	3	1.75		42,750	0
126.....	3	2.25		47,500	9,800
127.....	3	2.25		47,500	9,800
128.....	3	2.00		42,750	0
129.....	3	2.00		31,468	0
130.....	3	2.50		47,500	0
131.....	3	2.50		47,500	0
132.....	3	1.50		24,937	0
133.....	3	2.25		38,000	0
134.....	3	2.25		38,000	0
135.....	3	2.50	20.0	39,187	0
136.....	3	2.50		45,125	0
137.....	3	2.38		49,875	7,595
138.....	3	2.38		49,875	7,595
139.....	3	1.75		28,500	0
140.....	3	3.00		49,875	8,820
141.....	3	2.00		45,125	0
142.....	3	2.00		45,125	0

TABLE A-7. - Data for simulated drift in limestone--Continued

Break number	Feather angle, °	Depth of break, in	Weight of break material, kg	Force, lb	
				Radial	Axial
143.....	3	1.50		35,625	0
144.....	3	2.00		57,000	11,760
145.....	3	2.25		27,906	0
146.....	3	1.25		28,500	4,410
147.....	3	1.00		57,000	11,760
148.....	3	2.00		47,500	9,800
149.....	3	2.00	18.2	33,250	0
150.....	3	2.13		46,312	0
151.....	3	2.00		42,750	8,330
152.....	3	2.00		28,500	490
153.....	3	2.25		41,562	9,800
154.....	3	2.00		47,500	10,290
155.....	3	2.00		42,750	9,800
156.....	15	2.25		57,000	11,760
157.....	3	2.00		35,625	8,942
158.....	3	2.00	10.0	35,625	7,350
159.....	3	2.00		42,156	9,800
160.....	3	2.00		42,156	9,800
161.....	3	1.50		34,437	0
162.....	15	1.25		35,625	9,800
163.....	15	2.00	4.5	30,875	9,800
164.....	15	2.00		39,187	9,800
165.....	15	2.00		28,500	6,370
166.....	3	2.00		35,625	8,330
167.....	3	2.00		42,750	8,820
168.....	3	2.00		42,750	8,820
169.....	3	2.00		49,875	11,760
170.....	3	2.00		42,750	9,800
171.....	3	2.00		42,750	0
172.....	3	2.00		42,750	0
173.....	3	2.50		42,750	9,800
174.....	3	2.50		42,750	9,800
175.....	3	2.25		49,875	11,760
176.....	3	2.25		49,875	11,760
177.....	3	2.25	20.0	42,750	0
178.....	3	2.50		49,875	11,760
179.....	3	2.00		57,000	11,760
180.....	3	1.75		30,875	7,350
181.....	3	1.75		49,875	11,760
182.....	3	1.25		30,875	0
183.....	3	2.00		57,000	0
184.....	3	2.00		54,625	0
185.....	3	2.00		35,625	0
186.....	3	2.00		35,625	0
187.....	3	2.00		35,625	7,350
188.....	3	1.75		28.500	0

TABLE A-7. - Data for simulated drift in limestone--Continued

Break number	Feather angle, °	Depth of break, in	Weight of break material, kg	Force, lb	
				Radial	Axial
189.....	3	1.50		24,937	0
190.....	3	2.50		33,250	8,085
191.....	3	2.00		47,500	9,800
192.....	3	2.00		28,500	5,880
193.....	3	2.00		49,875	10,290
194.....	3	2.00		42,750	9,800
195.....	3	2.25	11.4	38,000	0
196.....	3	1.50		24,937	0
197.....	3	2.00		42,750	0
198.....	3	2.00		39,187	10,290
199.....	15	1.50		29,687	0
200.....	15	1.00		21,375	7,350
201.....	15	1.50		47,500	0
202.....	15	1.00		28,500	8,330
203.....	15	2.00		21,375	5,145
204.....	15	1.50	12.7	25,531	6,860
205.....	15	1.50		32,062	9,800
206.....	15	1.50		24,937	0
207.....	15	1.50		21,375	0
208.....	15	2.00		30,875	0
209.....	15	2.25		32,656	8,330
210.....	15	2.00	7.3	30,875	9,800
211.....	15	1.50		22,562	7,840
212.....	15	1.75		57,000	11,760
213.....	15	1.75		28,500	8,820
214.....	15	1.50		36,812	10,290
215.....	15	2.00		21,375	0
216.....	15	1.75		24,700	5,733
217.....	15	2.00		22,800	5,292
218.....	15	2.50	14.5	33,250	0
219.....	15	2.00		26,600	8,918
220.....	3	2.00		42,750	0
221.....	15	2.00		40,375	10,290
222.....	15	2.00		23,275	6,419
223.....	15	2.00		38,593	10,290

TABLE A-7. - Data for simulated drift in limestone--Continued

Break number	Feather angle, °	Depth of break, in	Weight of break material, kg	Force, lb	
				Radial	Axial
224.....	15	2.00		36,218	9,065
225.....	15	2.00		34,437	10,290
226.....	15	1.50		36,218	10,290
227.....	3	2.00		36,218	0
228.....	3	2.00		21,375	0
229.....	3	2.00		21,375	0
230.....	3	1.00		11,875	0
231.....	3	2.25		57,000	11,760
232.....	3	2.00		24,937	0
233.....	3	1.50	18.2	45,125	10,780
234.....	3	1.50		29,093	0
235.....	3	1.50		29,093	0
236.....	3	2.00		41,562	11,515
237.....	3	2.13		33,250	0
238.....	3	2.13		33,250	0
239.....	3	1.50		21,375	0
240.....	3	1.50		45,125	0
241.....	3	2.00		28,500	0
242.....	3	2.00		42,750	7,350
243.....	3	2.00		42,750	0
244.....	3	2.00		42,750	0
245.....	3	2.00		47,500	0
246.....	3	2.00		47,500	0
247.....	3	1.50	5.5	28,500	0
248.....	3	1.50		40,375	0
249.....	3	1.00		31,350	0
250.....	3	1.00		30,637	0
251.....	3	1.00		37,406	0
252.....	3	1.00		38,475	0
253.....	15	2.00		24,937	0
254.....	15	2.00		28,975	8,673
255.....	15	2.13	11.8	30,162	6,737
256.....	15	2.00		29,093	8,575
257.....	15	2.00		49,281	11,760
258.....	15	1.75		57,000	11,760

TABLE A-8. - Paired- and single-break data for limestone

Break number	Feather angle, °	Depth of break, in	Weight of break material, g	Force, lb		Spacing, in
				Radial	Axial	
PAIRED-BREAK DATA						
1A	3	1.38	523	21,375	5,630	5.00
1B	3	1.38		21,375	4,260	
2A	3	1.88	4,746	25,175	7,148	5.00
2B	3	1.88		27,788	7,589	
3A	3	2.25	1,914	35,863	9,939	5.69
3B	3	2.25		37,288	10,036	
4A	3	2.00	3,485	29,450	7,148	5.00
4B	3	2.00		28,500	7,589	
5A	3	1.25	1,423	18,050	5,581	4.25
5B	3	1.25		14,250	5,826	
6A	3	1.00	860	16,625	5,385	3.75
6B	3	1.00		10,687	1,958	
7A	3	1.25	1,917	12,350	4,410	3.75
7B	3	1.25		13,775	4,410	
SINGLE-BREAK DATA						
1	3	1.13	591	20,187	7,252	NAp
2	3	1.25	389	22,562	7,742	NAp
3	3	1.25	1,913	22,800	7,154	NAp
4	3	1.38	257	22,562	7,644	NAp
5	3	1.75	2,859	40,375	9,653	NAp
6	3	1.00	1,446	13,062	3,479	NAp
7	3	1.50	2,881	27,312	9,408	NAp
8	3	.75	140	10,925	1,568	NAp
9	3	1.88	3,337	28,737	9,702	NAp
10	3	1.88	2,956	41,800	9,800	NAp
11	3	1.50	1,916	21,375	8,575	NAp
12	3	1.00	228	12,112	6,125	NAp

NOTE.--For this comparison, paired-break data do not include tests conducted with spacing that was too large or small.

TABLE A-9. - Paired-break data for granite

Break number	Feather angle, °	Depth of break, in	Weight of break material, g	Force, lb		Spacing, in
				Radial	Axial	
1A	30	1.38	461	35,625	7,595	3.50
1B	30	1.38		35,625	7,595	
2A	30	1.25	2,697	35,625	8,575	3.00
2B	30	1.25		35,625	8,575	
3A	30	1.63	3,490	43,343	10,290	3.25
3B	30	1.63		43,343	10,290	
4A	30	1.25	1,022	28,500	7,105	3.25
4B	30	1.25		28,500	7,105	
5A	30	1.00	652	28,737	7,987	3.25
5B	30	1.00		28,737	7,987	
6A	30	1.63	1,650	45,600	10,780	3.63
6B	30	1.63		45,600	10,780	
7A	30	1.75	4,000	47,500	11,270	3.25
7B	30	1.75		47,500	11,270	

NOTE.--Single-break data for granite are shown in table A-5. For this comparison, paired-break data do not include tests conducted with spacing that was too large or small.

U.S. GOVERNMENT PRINTING OFFICE: 1987 - 605-017/60014

INT.-BU.OF MINES,PGH.,PA. 28412